scientific reports

OPEN

The cognitive triad network - oscillation - behaviour links individual differences in EEG theta frequency with task performance and effective connectivity

Andre Gómez-Lombardi[1,2]✉, Begoña Góngora Costa[2], Pavel Prado Gutiérrez[3], Pablo Muñoz Carvajal[4], Lucía Z. Rivera[5] & Wael El-Deredy[1,6]

We reconcile two significant lines of Cognitive Neuroscience research: the relationship between the structural and functional architecture of the brain and behaviour on the one hand and the functional significance of oscillatory brain processes to behavioural performance on the other. Network neuroscience proposes that the three elements, behavioural performance, EEG oscillation frequency, and network connectivity should be tightly connected at the individual level. Young and old healthy adults were recruited as a proxy for performance variation. An auditory inhibitory control task was used to demonstrate that task performance correlates with the individual EEG frontal theta frequency. Older adults had a significantly slower theta frequency, and both theta frequency and task performance correlated with the strengths of two network connections that involve the main areas of inhibitory control and speech processing. The results suggest that both the recruited functional network and the oscillation frequency induced by the task are specific to the task, are inseparable, and mark individual differences that directly link structure and function to behaviour in health and disease.

The quest of neuroscience is to discover how brain structure, function, and dynamics relate to behaviour. Two lines that run almost in parallel seek to associate structural and functional architecture with task performance[1–5]; and to understand the functional significance of the oscillatory processes observed at the level of EEG/MEG to behaviour[6,7]. Brain networks and brain oscillations are interconnected and play crucial roles in determining and driving behavioural outcomes. Brain networks refer to the functional and structural connections between different brain regions, while brain oscillations represent rhythmic patterns of neural activity in various frequency bands. The relationship between these two factors is bidirectional and dynamic. For instance, the strength and efficiency of brain connectivity can influence the synchronisation and coherence of brain oscillations, affecting cognitive processes and behaviour[8–11]. Nevertheless, brain oscillations can impact the functional connectivity between brain regions, shaping information flow and neural communication[10,12]. The direction of causality can vary depending on the context and cognitive task and remains a topic of inquiry. Different frequency bands of EEG oscillations are generally associated with specific functional connectivity patterns. For example, theta-band oscillations have been linked to long-range functional connectivity, particularly in tasks involving memory and attention. In contrast, gamma-band oscillations are related to local processing and information integration within specific brain regions[13]. Little is known about how an individual frequency within an EEG band might relate to the underlying network connectivity and behavioural performance.

Computational modelling studies show that the frequency of EEG oscillations depends on the network features. Notably, the frequency can be influenced by the resonant properties of the underlying neural networks[14,15],

[1]Brain Dynamics Laboratory, Universidad de Valparaíso, Valparaíso, Chile. [2]Centro de Investigación del Desarrollo en Cognición y Lenguaje, Universidad de Valparaíso, Valparaíso, Chile. [3]Escuela de Fonoaudiología, Facultad de Odontología y Ciencias de la Rehabilitación, Universidad San Sebastián, Santiago, Chile. [4]Centro para la Investigación Traslacional en Neurofarmacología, Escuela de Medicina, Facultad de Medicina, Universidad de Valparaíso, Valparaíso, Chile. [5]Centro Avanzado de Ingeniería Eléctrica y Electrónica, Universidad Técnica Federico Santa María, Valparaíso, Chile. [6]Department of Electronic Engineering, School of Engineering, Universitat de València, Valencia, Spain. ✉email: andre.gomez@uv.cl

where networks exhibit a preference for specific frequencies determined by their structural and functional features. For instance, resonance properties of the thalamocortical circuitry have been associated with the generation of alpha oscillations[16]. The size or spatial extent of the underlying network also influences the frequency of the oscillations. Large-scale networks involving multiple brain regions tend to generate lower-frequency oscillations, such as delta and theta, while local and smaller-scale networks display higher-frequency oscillations, such as beta and gamma[17,18]. The dynamics of network activity, including the synchronisation and coherence between different brain regions, can impact the frequency of EEG oscillations[19]. Network interactions and the balance between excitatory and inhibitory influences can shape the frequency characteristics of oscillatory activity[20–22].

To investigate the triangulation between network connectivity, individual oscillation frequency, and task performance, we exploit the variability in the three factors observed over the life span. Compared to younger adults, older adults exhibit altered functional connectivity patterns with consequences on oscillations and behaviour[23,24]. Age-related changes in brain oscillations are observed in most cognitive and behavioural domains: visuospatial memory[25], memory retrieval tasks[26], sensorimotor[27], attentional control[28], inhibitory control[29,30], among others. Most age-related associations between brain oscillations and cognitive performance are described in terms of the change in the power and phase of the oscillation[25–30], reflecting shifts in the synchronisation levels of the underlying networks.

The primary purpose of this study was to investigate the relationship between theta frequency and network connectivity while performing an auditory inhibitory control task in a sample of young and older adults. In addition, each participant completed a second task (i.e., auditory recognition task) to evaluate if theta frequency is task specific.

Inhibitory control refers to suppressing stimuli, thoughts, or behavioural responses incompatible or conflicting with a goal[31–33]. An example of inhibitory control is the Simon task, known for its sensitivity to the cognitive changes exhibited during ageing.[34–37] In the auditory version of this task[38], a conflict emerges when the required response (button press based on the heard word) diverges from the ear through which the stimulus is delivered. Performance on the incompatible/conflicting stimulus of the Simon task is shown to be associated with increased mid-frontal EEG theta power[39,40] as well as engagement of the prefrontal cortex[41].

We extracted the individual mid-frontal theta peak from EEG data and estimated effective connectivity within the theta band through dynamic causal modelling for induced responses[42] in a simplified four-node network. The nodes encompass the bilateral superior temporal gyrus, implicated in speech processing[43–46] and the bilateral Inferior frontal gyrus, recognised for their role in inhibitory control[40,41,47–50]. Finally, we conducted a correlation analysis between performance on the Simon task, the individual peaks of mid-frontal theta, and the estimated network connections.

Our study aimed to establish a comprehensive framework that links the brain network, EEG oscillation, and behaviour. By providing evidence to prove the interconnectedness of these three elements, we suggest that analysing this triad could be an effective approach to understanding behaviour by integrating relevant aspects of brain activity.

Results

Individual theta frequency (f_θ)—behavioural performance

The Simon effect[51,52] measures the difference in reaction time (RT) between responding to a compatible/congruent condition versus a conflicting incongruent condition. The size of the effect indicates the ease with which the conflict is resolved, such that a smaller Simon effect indicates better inhibitory control. Participants (n = 48, in two groups of older 60–73 yo and young 19–37 yo adults) pressed a button with the hand cued by the word left/right, independent of the ear where it is presented (e.g., left in left ear = congruent; left in right ear = incongruent).

The Simon effect was inversely correlated with the individual f_θ, extracted as the peak of the induced theta oscillation in mid-frontal electrodes, Fig. 1a, r_s (46) = − 0.42, p = 0.003. The f_θ was significantly lower (w(34.00) = 4.78, p < 0.001, d = 1.380) in the older adults (M = 4.05 Hz, Sd = 0.66) compared to younger adults (M = 5.49 Hz, Sd = 1.32), Fig. 1b. At the same time, in older adults, the Simon effect was significantly larger (U = 106, p < 0.001, r = − 0.63, Mdn older = 65.46, Mdn young = 31.99), Fig. 1c. For detailed analyses by condition and group, EEG time–frequency analyses, and topographies, see Supplementary Figs. S1 and S2 respectively. The older adults were slower but did not make any more errors than the younger adults, i.e., they succeeded in performing the task (Supplementary Fig. S1).

The power of the theta band was higher in the incongruent condition as previously documented[53–57], but the difference in theta power between the Incongruent and Congruent conditions did not correlate with the Simon effect (Supplementary Fig. S3).

Individual f_θ—effective connectivity

We analysed the correlation between f_θ and the network connections estimated by Dynamic Causal Modeling of the induced EEG responses (DCM-IR)[42]. Different DCM models were constructed and compared using Bayesian model selection (BMS); see Supplementary Figs. S6–S8. The winning model comprised the superior temporal gyrus (STG) and the inferior frontal gyrus (IFG), bilaterally and homotopically connected (Fig. 2a). The selection of nodes for constructing the DCM was guided by well-established literature highlighting the bilateral activation of the Superior Temporal Gyrus (STG) in speech processing[43–46] as well as the bilateral activation of the Inferior Frontal Gyrus (IFG) in inhibitory control[40,41,47–50]. These cognitive processes hold relevance in the context of the employed auditory version of the Simon task. Only these four nodes were selected to maintain a relevant yet simple network, if somewhat incomplete, to ensure robust identifiability.

The weights of the connections from the left STG to the right RSTG (LSTG-RSTG) and from the left STG to the left IFG (LSTG-LIFG) showed significant correlations with the f_θ. Specifically, LSTG-RSTG correlation was
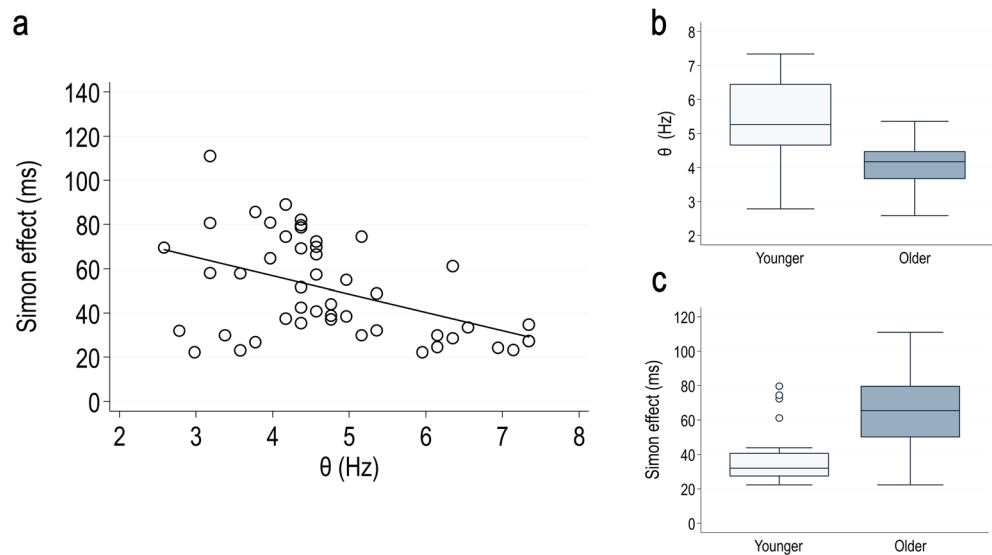
Fig. 1. Individual frontal theta frequency and Simon task behavioural performance. The Simon effect quantifies the temporal cost of successfully resolving spatial conflict caused by hearing a word in the ear opposite to its corresponding spatial meaning. A larger Simon effect indicates slower conflict resolution and, therefore, less inhibitory control[37,38,58]. (a) The Simon effect exhibited a negative correlation with f_θ, indicating that higher f_θ values were associated with a smaller Simon effect. (b) The f_θ was significantly lower in the older adults, coinciding with a considerably larger Simon effect (c), suggesting less efficient inhibitory control. A separate auditory recognition task was utilized to test the task dependency of f_θ. The task used the same stimuli with different instructions, resulting in significantly different f_θ (see Supplementary Fig. S4 for EEG time–frequency analyses and topographies). However, the significant correlation between task performance and frequency was maintained (Supplementary Fig. S5). This suggests that the individual f_θ is task dependent.
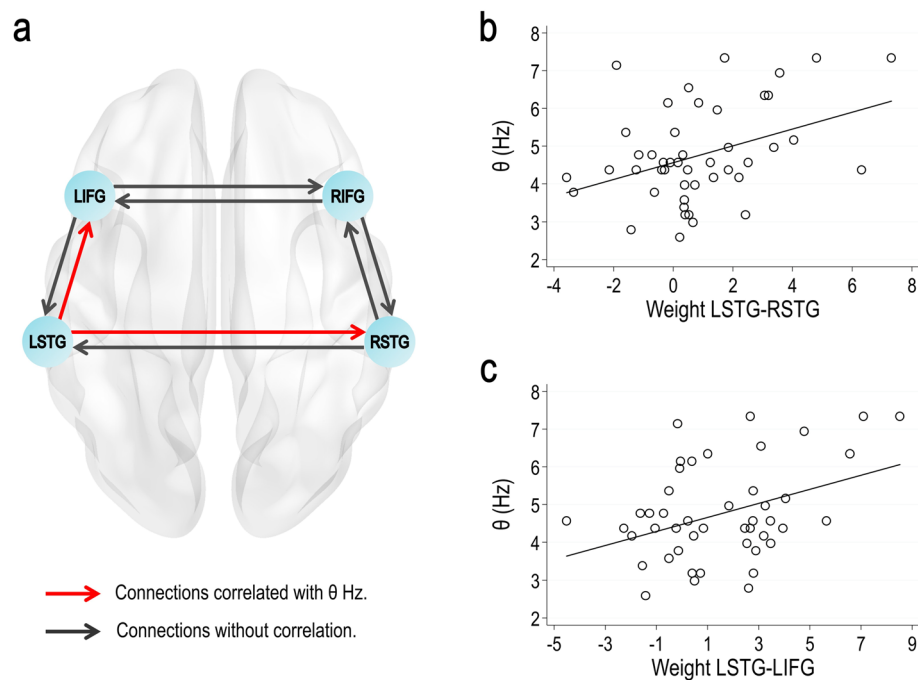
Fig. 2. Simon task frontal theta frequency correlates with network connections. (a) DCM winning model of the induced theta band (4–8 Hz) oscillation comprised the bilateral superior temporal gyrus (STG) and inferior frontal gyrus (IFG) with intra and interhemispheric connections (all modulated by the effects of congruent vs incongruent conditions). (b) Connection LSTG-RSTG correlated with the individual f_θ. (c) Connection LSTG-RIFG correlated with the individual f_θ.

$r_s(44) = 0.30$, p = 0.040 (Fig. 2b), and LSTG-LIFG correlation was $r(44)$ 0.39 p = 0.008 (Fig. 2c). In both cases, stronger network connections were associated with higher f_θ. To confirm the validity of the proposed network, using the same approach, we conducted a comparison with a separate group of models that included prefrontal sources other than the LIFG and RIFG, specifically focusing on the left and right anterior cingulate cortex (LAAC and RACC). The results showed that no connection weights of the winning model correlated with the frequency f_θ associated with the Simon task, as shown in Supplementary Fig. S9.

Behavioural performance—effective connectivity

Finally, we examined the association between behavioural performance in the Simon task and the connections of the networks depicted in Fig. 2a. Remarkably, the two connections that previously exhibited correlations with f_θ also correlated negatively with the Simon effect, specifically LSTG-RSTG (Fig. 3a, r(44) = − 0.32, p = 0.030) and LSTG-LIFG (Fig. 3b, r(44) = − 0.31, p = 0.037).

We ran additional analyses to exclude the possibility that the observed correlations are simply the result of general differences between younger and older participants, which would drive the correlation between any pair of observations. We tested the correlations between the Simon effect and the evoked (phase-locked) theta power and frequency and the induced (non-phase-locked) power. Despite the significant differences in evoked theta power and frequency between the age groups, they did not correlate with the Simon effect (Supplementary Fig. S10). Additionally, induced power did not correlate with the Simon effect ($r(46) = − 0.05$, p = 0.75), indicating that the Network-oscillation-behaviour triad is specific to the frequency of the induced oscillation.

Discussion

Our results provide evidence for the relationship of individual task-induced oscillation to the behavioural performance and neural connectivity in an auditory inhibitory control task considering two age groups. Higher f_θ was associated with faster conflict resolution, which was characteristic of younger adults. It is important to note that this pattern might differ with other tasks, such as working memory, where a lower f_θ frequency seems to be linked with enhanced performance[59]. Effective connectivity analysis revealed positive correlations between the individual f_θ and the strength of connections of the winning model explaining the induced theta oscillations during the Simon task, specifically LSTG-RSTG and LSTG-LIFG connections. Interestingly, the connections correlated with behavioural performance also showed a relationship with f_θ. This finding indicates a well-defined and consistent link between f_θ oscillation, effective connectivity patterns, and behavioural performance in the auditory Simon task. This 3-way link is specific to the induced oscillation, as it is not observed with the power of the oscillation or with the phase-locked activity, despite significant differences between the age groups.

Stimulus-related changes in ongoing oscillations result in both phase-locked (evoked) and variable latency (induced) components. The phase-locked component, associated with sensory processing, occurs immediately and consistently across trials, reflecting initial sensory responses[60]. In contrast, cognitive processing, such as interpreting word meaning or resolving a conflict, is variable, and introduces variable latency oscillations that are not as tightly time-locked to the stimulus[61]. Despite their variability, these cognitive oscillations remain rhythmic and reflect ongoing cognitive activities.

Cognitive neuroscience has focused on relating behaviour to two features of brain activity: oscillatory processes and the architecture of functional networks. Cognitive control has been related mainly to the theta oscillations[62,63], working memory to theta, alpha, and gamma oscillations[64,65], selective attention to theta, alpha and alpha/beta bands[66,67], among others. Nevertheless, triangulation of the findings from the three areas, behaviour, network connectivity, and oscillatory frequency, has remained relatively unexplored.

Induced responses represent changes in frequency-specific neural activity that occurs in response to certain cognitive processes or internal states, rather than in direct response to an external stimulus[68,69]. Power has been one of the most widely used parameters to report changes in brain dynamics in cognitive tasks[70–75]. In contrast, the individual oscillation frequency has been largely underexploited. Our research conceptually agrees with
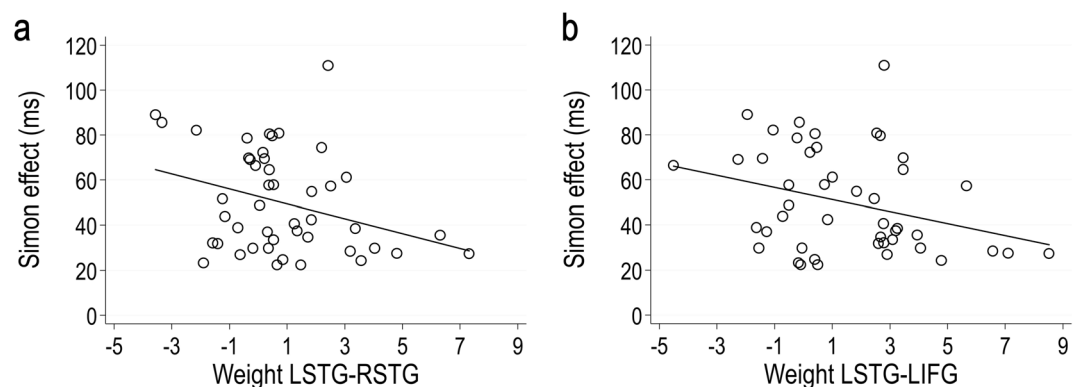
Fig. 3. Behavioural performance correlates with network connectivity. (**a**) Correlation between LSTG-RSTG and Simon effect. (**b**) Correlation between LSTG-LIFG and Simon effect. Stronger connectivity was associated with a smaller Simon effect, indicating improved conflict resolution and enhanced inhibitory control.

other studies relating it to cognitive tasks[76–78]. Specifically, the peak frequency of theta and alpha bands have been related to working memory capacity, where an increase in the peak of these frequencies correlates with memory load[77]. In addition, it has been demonstrated that the peak of theta adaptively shifts towards optimal frequency depending on task demands. This shift has been shown to correlate with behavioural performance[78].

We examined the capacity of peak frequency to account for alterations exhibited by older adults in both local and global functional connectivity[24,79]. The significant difference observed in behavioural performance and f_θ frequency between younger and older adults during the Simon task highlights the undeniable influence of ageing on brain dynamics and, consequently, cognitive control. The decrease in f_θ in the older adult group (Fig. 2b) could potentially indicate a change in the communication patterns between brain areas recruited for conflict resolution.

In our study, even under less than perfect conditions, such as using the individual brain anatomy of each subject to infer the neural generators and their interconnections, the connections between LSTG-RSTG and LSTG-LIFG exhibited a notable correlation with frequency (Fig. 2b and c). A weaker connection was related to a longer time to conflict resolution (Fig. 3a and b). Based on the evidence relating theta oscillation to the Simon task[39,40,80] and using induced-response DCM, we showed the variation of frequency with task performance and network connectivity. Utilising individual brain anatomy would enhance the specificity of these estimates, enabling the detection of stronger relationships between frequency and connectivity, as well as connectivity and behaviour. To emphasize the specificity of our proposed network, correlations were observed only between STG and IFG, but not with the ACC, an easily detectable EEG source, commonly related to cognitive control[81,82].

Considering that low frequencies have been associated with more extensive networks[14], the decrease in f_θ observed in older people might indicate the activation of a compensatory mechanism involving areas not engaged in younger adults for conflict resolution in the context of the Simon task. This idea is compatible with that proposed by compensation related utilisation of neural circuits hypothesis (CRUNCH) and hemispheric asymmetry reduction model (HAROLD) in older adults[34,83,84]. The different compensatory brain mechanisms in healthy ageing are intended to preserve cognitive performance[85]. Nonetheless, maintaining accuracy is counterbalanced by the extended temporal demand necessary for conflict resolution in the Simon task. This phenomenon is consistent with the processing speed theory[86,87], which states that ageing is associated with reducing the speed at which numerous processing operations can be executed.

To summarise, in network neuroscience, the causal relationship brain oscillations and neural networks is difficult to establish. There are two perspectives on this relationship: one posits oscillations as a consequence of network structural connectivity[14,88–90], shaping synchronised neural activity; the other argues synchronised oscillations play a causal role in shaping functional dynamics[91–93]. Our results suggest a likely bidirectional and dynamic relationship. Structural connectivity provides an anatomical substrate for neural interactions, while functional connectivity reflects dynamic coordination. Oscillations may emerge due to network organisation and, reciprocally, influence functioning through mechanisms like phase synchronisation and frequency-specific communication.

Impact

The present study uses a network science approach to link behavioural performance, brain oscillations, and connectivity. The evidence of this relationship can be used as a framework for future studies to understand the scope of the use of personalised oscillatory parameters (i.e., individual frequency) in non-invasive brain stimulation. A possible application of this assumption is in the context of neural entrainment since this mechanism has been shown to improve performance in different cognitive domains[94–96], adjusting neural oscillatory activity to external input, even in the supramodal modality[97]. Future studies are required to establish the feasibility of optimising behavioural performance through precisely calibrating stimulation frequencies meticulously tailored to individual characteristics and the targeted cognitive domain.

Material and methods

All experimental procedures followed the principles established in the 1964 Declaration of Helsinki and its subsequent revisions. The study and informed consent were approved by the Ethical Committee of the Medical School of the Universidad de Valparaíso (Permission No. 15/2021), according to international standards.

Participants

Fifty-four people, recruited from the population via adverts, were informed about the purposes and procedures of the study and consented to participate. Informed consent was obtained from all subjects involved in the study. Six participants were excluded due to hearing loss (n = 1), psychiatric history (n = 2), and significant artefacts in their EEG recordings (n = 3). The reported analyses consisted of 48 participants: Twenty-four younger adults aged 19–37 (12 females; mean age = 25.00; SD = 5.23) and 24 older adults aged 60–73 years (12 females; mean age 64.66; SD = 3.23).

All participants were Spanish speakers, self-reported as right-handed, and with post-secondary education. In a clinical interview, they reported good health, with no history of neurological or psychiatric disorder, and not having hearing difficulties. None of the participants was under medication for the central nervous system. All participants passed a screening audiometry, ensuring adequate hearing to perform the task. We considered a pure tone average (PTP) ≤ 20 dB HL for the younger group, while for the older group, a PTP ≤ 30 dB HL considering normal age-related changes in hearing.

Participants were screened for cognitive impairment. The older group was evaluated using the Montreal Cognitive Assessment (MoCA), while the younger group was assessed with the Mini-Mental State Examination (MMSE). Both instruments have been normatively validated for the Chilean population, with cut-off scores

of ≥ 29 points on the MMSE[98] for the younger group and ≥ 22 points on the MoCA[99] for older adults, discarding any cognitive impairment.

Experimental task and procedure

The study was designed as a single session comprising two tasks: The main inhibitory control task and a secondary auditory recognition task. The latter task was included to demonstrate that each task has a characteristic theta frequency related to individual behavioural performance, regardless of the cognitive domain under study.

The order in which the participants performed the tests was counterbalanced entirely. The same experimental setup was used for both tasks and consisted of a modification of the original Simon task[38]. The test was designed and programmed in E-prime 3 software.

Stimuli

The stimuli were created based on two monaural Spanish words, "*izquierda*" and "*derecha*" (in English left and right). The words had a low or high-pitched voice and were presented in the left or right ear.

To create the stimuli, a neutral pitched voice for each word was recorded in an acoustic chamber at a sampling rate of 44.1 kHz. The recorded voice was then modified by 24% towards both high and low pitch with Audacity software v3.1.3.

The stimuli can be classified as congruent or incongruent in the Simon task and non-target or target in the auditory recognition task. In the congruent condition, there was a match between the word [Left/Right] and the ear where it was presented. In the incongruent condition, the word did not match the ear. In the target condition, participants responded to a specific voice pitch (High or low, counterbalanced between subjects). In contrast, in the non-target condition, the response was to be omitted.

Procedure

Participants sat comfortably in an acoustics chamber, one meter in front of a screen for reading the instructions. To hear and respond to the stimuli, subjects used headphones (Shure SRH440) and a response box (Chronos, PST) with the leftmost and rightmost buttons activated for responses. The instruction for the Simon task was to press the correct button according to the word heard [Left/Right], irrespective of the ear to which it is presented or the pitch of the voice.

The instruction for the Auditory Recognition task was to press the right button with the right thumb only if the voice of the word had the target pitch previously defined, regardless of the word heard and the ear in which it was presented. The high and low pitches of target voices were counterbalanced for all participants.

Before each task, a practice phase (72 trials) was performed to ensure understanding of the tests. The stimuli were presented at an intensity of ~ 65 dBA. The stimuli were presented randomly while avoiding long sequences of consecutive presentations of identical stimuli. Tasks were organised in 4 blocks with breaks in between. There were 480 trials (240 by condition: Congruent/Incongruent for the Simon task and Target/No Target for the Recognition task).

Each trial started with 600 ms fixation; the stimulus lasted ~ 300 ms, followed by a window of 1000 ms for responding. Participants were instructed to respond as fast as they could. A random period of 400 to 650 ms was considered for the inter-trial interval.

EEG recording and pre-processing

EEG was continuously recorded using the 64-channel BioSemi ActiveTwo system (BioSemi Inc., Heerlen, Netherlands) with a 24-bit analog-to-digital conversion at a sampling rate of 4096 Hz. Blinks and eye movements were recorded with four electrodes placed on the outer part of the left and right eyes and above and below the left eye.

The EEG data were processed offline using the EEGLAB[100] toolbox for MATLAB (MathWorks, Natick, MA, USA). A visual review of the continuous recording was performed to eliminate traces with significant artefacts. The data was filtered between 0.1 and 100 Hz and then down sampled to 512 Hz. An Artifact Subspace Reconstruction (ASR) was used, considering a cutoff parameter k = 20[101]. Recordings were re-referenced to the average of all scalp electrodes. Bad electrodes were interpolated using spherical spline interpolation, with an average of approximately 3 ± 2 electrodes per participant. Details are provided in the Supplementary Information.

An independent component analysis (ICA) was implemented to remove artefacts such as eye blinks, ocular movements, and muscular noise. Finally, the data were epoched with a time window of 1.8 s (0.5 s pre stimulus and 1.3 s post stimulus, around the time stimulus onset), considering only correct responses.

Time frequency analysis

The time frequency (TF) analyses were performed in each channel using continuous wavelet transform for the pre-processing and segmented data for each condition. The TF power was computed using a complex Morlet wavelet of 4 cycles at 1 Hz, increasing logarithmically to 13 cycles at 90 Hz over single trials, thus balancing between temporal and frequency precision as a function of the frequency of the wavelet[102]. A high resolution of 0.2 Hz was established, with 450 frequency bins linearly distributed from 1 to 90 Hz to observe the entire frequency range from delta to gamma bands. For a more precise analysis of the theta band frequency, following an initial overview of the entire frequency range, the frequency window was narrowed down to the range between 1 and 12 Hz to extract the f_θ.

We analysed the data as induced response, i.e. as a jittered non-phase locked response, acknowledging the difficulty in separating task-induced jittered response from a task-related change in ongoing oscillation[102]. Total TF power contains evoked (phase-locked) and induced (non phase-locked) activity for each time point across the epoch (− 500 to 1300 ms). It is obtained through the ratio (in decibels, dB) of the power at each time point relative

to the baseline time (− 300 to − 100 ms). First, to obtain the non-phase-locked power, it was necessary to subtract the event-related potential (ERP) of each electrode and trial type from the corresponding individual epochs of the EEG data. Then, the complex Morlet wavelet was applied according to the abovementioned procedure.

TF data was plotted at five mid-frontal electrodes (FC3, FC1, FCz, FC2, and FC4). A region of interest was established around the area of highest power in the theta frequency band for each of the conditions of the inhibitory control and auditory recognition tasks (Supplementary Figs. S2 and S4, respectively). Within these areas of interest, the maximum power value was extracted, representing the f_θ associated with each condition and task studied. It is important to highlight that, in certain instances, the f_θ was observed to fall outside the typical bounds of the theta band (3–7 Hz). Some subjects exhibited values slightly below 3 Hz, indicative of a slowing in the theta band, primarily attributed to changes in brain networks due to ageing.

Dynamic causal modelling

DCM IR has been widely employed in numerous research studies, demonstrating its efficacy in exploring the dynamic relationships among brain regions[42,103–106]. In this study, DCM IR was used to determine effective connectivity in the theta band among sources related to the Simon task. The sources included in DCM-IR correspond to bilateral superior temporal gyrus (STG; left [− 61 − 32 8], right [59 − 25 8]) and bilateral inferior frontal gyrus (IFG; left [− 46 20 8], right [46 20 8]). Source locations (MNI coordinates) were obtained from a previous study using such sources[107]. Equivalent current dipoles (ECD) were used to extract the source data. To focus the analysis on the theta band, the spectral density from 1 to 8 Hz (minimum allowable range in SPM) was estimated on the high pass filtered EEG data (3 Hz). A Morlet wavelet transform was used with a coefficient, k = 8, over a 0–1000 ms time window. We reduced the dimensionality of the spectra to a single principal frequency component (1 mode) by singular value decomposition. The decision to use one mode was motivated by our interest in a single frequency band (theta) and not in cross-frequency interaction among sources. Only linear connections were considered in inverted models, as our primary focus was to examine the influence of frequency dynamics in one source on the dynamics at the corresponding frequencies in other sources.

Dynamic Causal Modeling (DCM) of the induced responses is a tool for studying and modelling interactions between distinct brain regions concerning spectral responses[42,103]. Since its introduction, DCM has been widely employed in numerous research studies, demonstrating its efficacy in exploring the dynamic relationships among brain regions[103–106]. In EEG connectivity analysis, it is challenging to definitively ensure that the reconstructed signals reflect only the activity of the selected nodes without any contamination from neighbouring areas. Utilising individual brain anatomy, as opposed to the average template we used, would enhance the specificity of estimates by allowing the precise selection of coordinates for the brain areas proposed in our brain network model.

Bayesian model selection

The model with the highest exceedance probability was considered the winning model. To test which model best explains the data obtained in the Simon task in two age groups (younger and older adults), the Bayesian model selection (BMS) with random effects (RFX) was conducted in two main stages. First, to determine the best structural family and model in the Simon task in each age group, we compared 24 alternative models (12 forward and 12 forward backward) grouped into five families according to their interhemispheric connections between homotopic sources (Supplementary Fig. S6). Once all the proposed structural models were inverted and the winning family was determined, a new BMS was conducted, testing only the models in the winning family. The winning family and model were selected according to their exceedance probability (Supplementary Fig. S7).

The next stage was to determine which connections of the winning structural model could be modulated by the congruent vs incongruent condition of the Simon task. We considered and inverted 24 models with different interhemispheric modulation patterns (12 forward and 12 backward), divided into five families according to the different modulations of interhemispheric connections between homotopic sources (Supplementary Fig. S6). As in the previous stage, once all the models with modulations were inverted and the winning family was determined, a new BMS was conducted, testing only the models in the winning family. The winning family and model were selected according to their exceedance probability (Supplementary Fig. S8), obtaining the final model that best explains the data recorded during the Simon task (Fig. 3a).

Data analysis

For all analyses, parametric statistical tests were employed based on satisfying specific assumptions. If any of them were not met, corrections were applied, or alternative tests were used. Only the correct answers were considered, except for HR analyses. It was considered a significance level (alpha) of 0.05 for all tests.

Behavioural performance

The Mann–Whitney test was employed to compare the Simon effect between younger and older adults, as the normality assumption was not satisfied. In addition, a two-way mixed ANOVA was employed to assess the main effects of condition, age groups, and their interaction on response times and hit rate. Post Hoc tests were used to uncover specific differences between three or more group means when ANOVA was significant.

In the auditory recognition task, a t-test was used to compare reaction times and Hit rate of target condition between young and older adults.

Theta frequency

In the analyses that considered f_θ, we use the incongruent condition for the Simon task and the target condition for the auditory recognition task since both conditions represent the main conditions of each task. Due to the lack of homogeneity in variances, a Welch t-test was considered to compare the frequency of younger and older

adults in the Simon task. A Mann–Whitney test was employed to compare the frequency of younger and older adults, as the normality assumption was not satisfied.

To compare the induced peak f_θ of the Simon task to the induced peak f_θ of the Auditory recognition task, the conditions of both tasks (congruent and incongruent for the Simon task, and Target and No target for the Auditory recognition task) were collapsed, and a paired samples t-test was performed (Supplementary Fig. S5).

In addition, we used the evoked peak theta f_θ from the Simon task to determine if the relationship with behaviour is specific to the induced oscillation.

Power analyses
A two-way mixed ANOVA was employed to assess the main effects of condition, age groups, and their interaction on induced power. To evaluate the difference in the power of the Simon effect (incongruent power − congruent power) between age groups, an independent t-test was performed.

Relationship between f_θ—effective connectivity and behavior
Correlation analyses were performed to establish the relationship between f_θ, effective connectivity, and behavioural performance. Two participants were excluded from the analysis because their effective connectivity values in any of the winning model connections deviated more than ± 3.5 SD from the mean. Depending on whether the pairwise normality assumption was met, Pearson's r or Spearman's rho correlation coefficient was used, respectively.

Data availability
The data that support the findings of this study are available from the dataset included in Supplementary information.

References
1. Albert, K. M., Potter, G. G., Boyd, B. D., Kang, H. & Taylor, W. D. Brain network functional connectivity and cognitive performance in major depressive disorder. *J. Psychiatr. Res.* **110**, 51–56 (2019).
2. Parris, B. A. et al. An fMRI study of response and semantic conflict in the stroop task. *Front. Psychol.* **10**, 2426 (2019).
3. Rosenberg, M. D. et al. Behavioral and neural signatures of working memory in childhood. *J. Neurosci.* **40**, 5090–5104 (2020).
4. Won, J., Alfini, A. J., Weiss, L. R., Callow, D. D. & Smith, J. C. Brain activation during executive control after acute exercise in older adults. *Int. J. Psychophysiol.* **146**, 240–248 (2019).
5. Wylie, G. R., Yao, B., Genova, H. M., Chen, M. H. & DeLuca, J. Using functional connectivity changes associated with cognitive fatigue to delineate a fatigue network. *Sci. Rep.* **10**, 21927 (2020).
6. Klimesch, W. The frequency architecture of brain and brain body oscillations: An analysis. *Eur. J. Neurosci.* **48**, 2431–2453 (2018).
7. Thut, G., Miniussi, C. & Gross, J. The functional importance of rhythmic activity in the brain. *Curr. Biol.* **22**, R658–R663 (2012).
8. Fries, P. Rhythms for cognition: Communication through coherence. *Neuron* **88**, 220–235 (2015).
9. Paneri, S. & Gregoriou, G. G. Top-down control of visual attention by the prefrontal cortex. Functional specialization and long-range interactions. *Front. Neurosci.* **11**, 545 (2017).
10. Salinas, E. & Sejnowski, T. J. Correlated neuronal activity and the flow of neural information. *Nat. Rev. Neurosci.* **2**, 539–550 (2001).
11. Varela, F., Lachaux, J.-P., Rodriguez, E. & Martinerie, J. The brainweb: Phase synchronization and large-scale integration. *Nat. Rev. Neurosci.* **2**, 229–239 (2001).
12. Cabral, J., Hugues, E., Sporns, O. & Deco, G. Role of local network oscillations in resting-state functional connectivity. *NeuroImage* **57**, 130–139 (2011).
13. Ward, L. M. Synchronous neural oscillations and cognitive processes. *Trends Cogn. Sci.* **7**, 553–559 (2003).
14. Lea-Carnall, C. A., Montemurro, M. A., Trujillo-Barreto, N. J., Parkes, L. M. & El-Deredy, W. Cortical resonance frequencies emerge from network size and connectivity. *PLoS Comput. Biol.* **12**, e1004740 (2016).
15. Voloh, B. & Womelsdorf, T. A role of phase-resetting in coordinating large scale neural networks during attention and goal-directed behavior. *Front. Syst. Neurosci.* https://doi.org/10.3389/fnsys.2016.00018 (2016).
16. Hindriks, R. & Van Putten, M. J. A. M. Thalamo-cortical mechanisms underlying changes in amplitude and frequency of human alpha oscillations. *NeuroImage* **70**, 150–163 (2013).
17. Nunez, P. L. Toward a quantitative description of large-scale neocortical dynamic function and EEG. *Behav. Brain Sci.* **23**, 371–398 (2000).
18. Von Stein, A. & Sarnthein, J. Different frequencies for different scales of cortical integration: From local gamma to long range alpha/theta synchronization. *Int. J. Psychophysiol.* **38**, 301–313 (2000).
19. Hipp, J. F., Engel, A. K. & Siegel, M. Oscillatory synchronization in large-scale cortical networks predicts perception. *Neuron* **69**, 387–396 (2011).
20. Pfeffer, T. et al. Circuit mechanisms for the chemical modulation of cortex-wide network interactions and behavioral variability. *Sci. Adv.* **7**, eabf5620 (2021).
21. Schirner, M., McIntosh, A. R., Jirsa, V., Deco, G. & Ritter, P. Inferring multi-scale neural mechanisms with brain network modelling. *elife* **7**, e28927 (2018).
22. Whittington, M. A., Traub, R. D., Kopell, N., Ermentrout, B. & Buhl, E. H. Inhibition-based rhythms: Experimental and mathematical observations on network dynamics. *Int. J. Psychophysiol.* **38**, 315–336 (2000).
23. Ishii, R. et al. Healthy and pathological brain aging: From the perspective of oscillations, functional connectivity, and signal complexity. *Neuropsychobiology* **75**, 151–161 (2018).
24. Sala-Llonch, R., Bartrés-Faz, D. & Junqué, C. Reorganization of brain networks in aging: A review of functional connectivity studies. *Front. Psychol.* https://doi.org/10.3389/fpsyg.2015.00663 (2015).
25. Rondina, R. et al. Age-related changes to oscillatory dynamics in hippocampal and neocortical networks. *Neurobiol. Learn. Mem.* **134**, 15–30 (2016).
26. Strunk, J., James, T., Arndt, J. & Duarte, A. Age-related changes in neural oscillations supporting context memory retrieval. *Cortex* **91**, 40–55 (2017).

27. Dushanova, J. & Christov, M. The effect of aging on EEG brain oscillations related to sensory and sensorimotor functions. *Adv. Med. Sci.* **59**, 61–67 (2014).
28. Huizeling, E., Wang, H., Holland, C. & Kessler, K. Changes in theta and alpha oscillatory signatures of attentional control in older and middle age. *Eur. J. Neurosci.* **54**, 4314–4337 (2021).
29. Schmiedt-Fehr, C., Mathes, B. & Basar-Eroglu, C. Alpha brain oscillations and inhibitory control: A partially preserved mechanism in healthy aging?. *J. Psychophysiol.* **23**, 208–215 (2009).
30. Schmiedt-Fehr, C., Mathes, B., Kedilaya, S., Krauss, J. & Basar-Eroglu, C. Aging differentially affects alpha and beta sensorimotor rhythms in a go/nogo task. *Clin. Neurophysiol.* **127**, 3234–3242 (2016).
31. Diamond, A. Executive functions. *Annu. Rev. Psychol.* **64**, 135–168 (2013).
32. Nigg, J. T. On inhibition/disinhibition in developmental psychopathology: Views from cognitive and personality psychology and a working inhibition taxonomy. *Psychol. Bull.* **126**, 220–246 (2000).
33. Tiego, J., Testa, R., Bellgrove, M. A., Pantelis, C. & Whittle, S. A hierarchical model of inhibitory control. *Front. Psychol.* **9**, 1339 (2018).
34. Kang, W., Wang, J. & Malvaso, A. Inhibitory control in aging: The compensation-related utilization of neural circuits hypothesis. *Front. Aging Neurosci.* **13**, 771885 (2022).
35. Kubo-Kawai, N. & Kawai, N. Elimination of the enhanced Simon effect for older adults in a three-choice situation: Ageing and the Simon effect in a go/no-go Simon task. *Q. J. Exp. Psychol.* **63**, 452–464 (2010).
36. Lubbe, R. H. J. & Verleger, R. Aging and the Simon task. *Psychophysiology* **39**, 100–110 (2002).
37. Proctor, R. W., Pick, D. F., Vu, K.-P.L. & Anderson, R. E. The enhanced Simon effect for older adults is reduced when the irrelevant location information is conveyed by an accessory stimulus. *Acta Psychol.* **119**, 21–40 (2005).
38. Simon, J. R. & Rudell, A. P. Auditory S-R compatibility: The effect of an irrelevant cue on information processing. *J. Appl. Psychol.* **51**, 300–304 (1967).
39. Cao, Y., Cao, X., Yue, Z. & Wang, L. Temporal and spectral dynamics underlying cognitive control modulated by task-irrelevant stimulus-response learning. *Cogn. Affect. Behav. Neurosci.* **17**, 158–173 (2017).
40. Cespón, J., Hommel, B., Korsch, M. & Galashan, D. The neurocognitive underpinnings of the Simon effect: An integrative review of current research. *Cogn. Affect. Behav. Neurosci.* **20**, 1133–1172 (2020).
41. van Campen, A. D., Kunert, R., van den Wildenberg, W. P. M. & Ridderinkhof, K. R. Repetitive transcranial magnetic stimulation over inferior frontal cortex impairs the suppression (but not expression) of action impulses during action conflict. *Psychophysiology* **55**, e13003 (2018).
42. Chen, C. C., Kiebel, S. J. & Friston, K. J. Dynamic causal modelling of induced responses. *NeuroImage* **41**, 1293–1312 (2008).
43. Bhaya-Grossman, I. & Chang, E. F. Speech computations of the human superior temporal gyrus. *Annu. Rev. Psychol.* **73**, 79–102 (2022).
44. Poeppel, D. The neuroanatomic and neurophysiological infrastructure for speech and language. *Curr. Opin. Neurobiol.* **28**, 142–149 (2014).
45. Yi, H. G., Leonard, M. K. & Chang, E. F. The encoding of speech sounds in the superior temporal gyrus. *Neuron* **102**, 1096–1110 (2019).
46. Zatorre, R. J., Evans, A. C., Meyer, E. & Gjedde, A. Lateralization of phonetic and pitch discrimination in speech processing. *Science* **256**, 846–849 (1992).
47. Boen, R., Raud, L. & Huster, R. J. Inhibitory control and the structural parcelation of the right inferior frontal gyrus. *Front. Hum. Neurosci.* **16**, 787079 (2022).
48. Kharitonova, M., Martin, R. E., Gabrieli, J. D. E. & Sheridan, M. A. Cortical gray-matter thinning is associated with age-related improvements on executive function tasks. *Dev. Cogn. Neurosci.* **6**, 61–71 (2013).
49. Li, Q. et al. Conflict detection and resolution rely on a combination of common and distinct cognitive control networks. *Neurosci. Biobehav. Rev.* **83**, 123–131 (2017).
50. Swick, D., Ashley, V. & Turken, A. U. Left inferior frontal gyrus is critical for response inhibition. *BMC Neurosci.* **9**, 102 (2008).
51. Lu, C.-H. & Proctor, R. W. The influence of irrelevant location information on performance: A review of the Simon and spatial Stroop effects. *Psychon. Bull. Rev.* **2**, 174–207 (1995).
52. Simon, J. R. The effects of an irrelevant directional cue on human information processing. In *Advances in Psychology* vol. 65 31–86 (Elsevier, 1990).
53. Cohen, M. X. & Ridderinkhof, K. R. EEG source reconstruction reveals frontal-parietal dynamics of spatial conflict processing. *PLoS ONE* **8**, e57293 (2013).
54. Gulbinaite, R., Van Rijn, H. & Cohen, M. X. Fronto-parietal network oscillations reveal relationship between working memory capacity and cognitive control. *Front. Hum. Neurosci.* https://doi.org/10.3389/fnhum.2014.00761 (2014).
55. Nigbur, R., Ivanova, G. & Stürmer, B. Theta power as a marker for cognitive interference. *Clin. Neurophysiol.* **122**, 2185–2194 (2011).
56. Vissers, M. E., Ridderinkhof, K. R., Cohen, M. X. & Slagter, H. A. Oscillatory mechanisms of response conflict elicited by color and motion direction: An individual differences approach. *J. Cogn. Neurosci.* **30**, 468–481 (2018).
57. Wang, K., Li, Q., Zheng, Y., Wang, H. & Liu, X. Temporal and spectral profiles of stimulus–stimulus and stimulus–response conflict processing. *NeuroImage* **89**, 280–288 (2014).
58. Simon, J. R. & Small, A. Jr. Processing auditory information: Interference from an irrelevant cue. *J. Appl. Psychol.* **53**, 433 (1969).
59. Wolinski, N., Cooper, N. R., Sauseng, P. & Romei, V. The speed of parietal theta frequency drives visuospatial working memory capacity. *PLoS Biol.* **16**, e2005348 (2018).
60. Makeig, S. et al. Dynamic brain sources of visual evoked responses. *Science* **295**, 690–694 (2002).
61. Tallon-Baudry, C. Oscillatory gamma activity in humans and its role in object representation. *Trends Cogn. Sci.* **3**, 151–162 (1999).
62. Cavanagh, J. F. & Frank, M. J. Frontal theta as a mechanism for cognitive control. *Trends Cogn. Sci.* **18**, 414–421 (2014).
63. Tafuro, A., Ambrosini, E., Puccioni, O. & Vallesi, A. Brain oscillations in cognitive control: A cross-sectional study with a spatial stroop task. *Neuropsychologia* **133**, 107190 (2019).
64. Scharinger, C., Soutschek, A., Schubert, T. & Gerjets, P. Comparison of the working memory load in N-back and working memory span tasks by means of EEG frequency band power and P300 amplitude. *Front. Hum. Neurosci.* **11**, (2017).
65. Wianda, E. & Ross, B. The roles of alpha oscillation in working memory retention. *Brain Behav.* **9**, e01263 (2019).
66. Foxe, J. J. & Snyder, A. C. The role of alpha-band brain oscillations as a sensory suppression mechanism during selective attention. *Front. Psychol.* https://doi.org/10.3389/fpsyg.2011.00154 (2011).
67. McDermott, T. J., Wiesman, A. I., Proskovec, A. L., Heinrichs-Graham, E. & Wilson, T. W. Spatiotemporal oscillatory dynamics of visual selective attention during a flanker task. *NeuroImage* **156**, 277–285 (2017).
68. *Induced Rhythms in the Brain*. (Birkhäuser Boston, 1992). https://doi.org/10.1007/978-1-4757-1281-0.
69. David, O., Kilner, J. M. & Friston, K. J. Mechanisms of evoked and induced responses in MEG/EEG. *NeuroImage* **31**, 1580–1591 (2006).
70. Helfrich, R. F. & Knight, R. T. Oscillatory dynamics of prefrontal cognitive control. *Trends Cogn. Sci.* **20**, 916–930 (2016).
71. Khader, P. H., Jost, K., Ranganath, C. & Rösler, F. Theta and alpha oscillations during working-memory maintenance predict successful long-term memory encoding. *Neurosci. Lett.* **468**, 339–343 (2010).

72. Lin, E. & Schmid, P. C. Does power increase attention to rewards? Examining the brain and behavior. *J. Exp. Soc. Psychol.* **101**, 104332 (2022).
73. Myers, J. C., Chinn, L. K., Sur, S. & Golob, E. J. Widespread theta coherence during spatial cognitive control. *Neuropsychologia* **160**, 107979 (2021).
74. Schmid, P. C., Kleiman, T. & Amodio, D. M. Power effects on cognitive control: Turning conflict into action. *J. Exp. Psychol. Gen.* **144**, 655–663 (2015).
75. Zavala, B. et al. Cognitive control involves theta power within trials and beta power across trials in the prefrontal-subthalamic network. *Brain* **141**, 3361–3376 (2018).
76. Ghazi, T. R., Blacker, K. J., Hinault, T. T. & Courtney, S. M. Modulation of peak alpha frequency oscillations during working memory is greater in females than males. *Front. Hum. Neurosci.* **15**, 626406 (2021).
77. Moran, R. J. et al. Peak frequency in the theta and alpha bands correlates with human working memory capacity. *Front. Hum. Neurosci.* https://doi.org/10.3389/fnhum.2010.00200 (2010).
78. Senoussi, M. et al. Theta oscillations shift towards optimal frequency for cognitive control. *Nat. Hum. Behav.* **6**, 1000–1013 (2022).
79. Coelho, A. et al. Reorganization of brain structural networks in aging: A longitudinal study. *J. Neurosci. Res.* **99**, 1354–1376 (2021).
80. Töllner, T. et al. Two independent frontal midline theta oscillations during conflict detection and adaptation in a simon-type manual reaching task. *J. Neurosci.* **37**, 2504–2515 (2017).
81. Friedman, N. P. & Robbins, T. W. The role of prefrontal cortex in cognitive control and executive function. *Neuropsychopharmacology* **47**, 72–89 (2022).
82. Cai, X. et al. The neural mechanisms of cognitive control in the category induction task. *Front. Psychol.* **13**, 743178 (2022).
83. Cabeza, R. Hemispheric asymmetry reduction in older adults: The HAROLD model. *Psychol. Aging* **17**, 85–100 (2002).
84. Reuter-Lorenz, P. A. & Cappell, K. A. Neurocognitive aging and the compensation hypothesis. *Curr. Dir. Psychol. Sci.* **17**, 177–182 (2008).
85. Martins, R., Joanette, Y. & Monchi, O. The implications of age-related neurofunctional compensatory mechanisms in executive function and language processing including the new Temporal Hypothesis for Compensation. *Front. Hum. Neurosci.* https://doi.org/10.3389/fnhum.2015.00221 (2015).
86. Salthouse, T. A. The processing-speed theory of adult age differences in cognition. *Psychol. Rev.* **103**, 403 (1996).
87. Salthouse, T. A. Aging and measures of processing speed. *Biol. Psychol.* **54**, 35–54 (2000).
88. Buzsáki, G. *Rhythms of the Brain*. (Oxford University Press, 2006). https://doi.org/10.1093/acprof:oso/9780195301069.001.0001.
89. Deco, G. & Kringelbach, M. L. Great expectations: Using whole-brain computational connectomics for understanding neuropsychiatric disorders. *Neuron* **84**, 892–905 (2014).
90. Sporns, O. The human connectome: A complex network. *Ann. N. Y. Acad. Sci.* **1224**, 109–125 (2011).
91. Fries, P. A mechanism for cognitive dynamics: Neuronal communication through neuronal coherence. *Trends Cogn. Sci.* **9**, 474–480 (2005).
92. Singer, W. Neuronal synchrony: A versatile code for the definition of relations?. *Neuron* **24**, 49–65 (1999).
93. Womelsdorf, T. et al. Modulation of neuronal interactions through neuronal synchronization. *Science* **316**, 1609–1612 (2007).
94. Albouy, P., Weiss, A., Baillet, S. & Zatorre, R. J. Selective entrainment of theta oscillations in the dorsal stream causally enhances auditory working memory performance. *Neuron* **94**, 193-206.e5 (2017).
95. Köster, M., Martens, U. & Gruber, T. Memory entrainment by visually evoked theta-gamma coupling. *NeuroImage* **188**, 181–187 (2019).
96. Riecke, L., Formisano, E., Sorger, B., Başkent, D. & Gaudrain, E. Neural entrainment to speech modulates speech intelligibility. *Curr. Biol.* **28**, 161-169.e5 (2018).
97. Albouy, P., Martinez-Moreno, Z. E., Hoyer, R. S., Zatorre, R. J. & Baillet, S. Supramodality of neural entrainment: Rhythmic visual stimulation causally enhances auditory working memory performance. *Sci. Adv.* **8**, eabj9782 (2022).
98. González-Hernández, J., Aguilara, L., Oporto, S., Araneda, L. & Vásquez, M. Normalización del Mini-Mental State Examination según edad y educación, para la población de Santiago de Chile. (2009).
99. Gaete, M. et al. Resultados estandarizados del Montreal Cognitive Assessment (MoCA) para cribado neurocognitivo en población chilena. *Neurología* https://doi.org/10.1016/j.nrl.2020.08.017 (2020).
100. Delorme, A. & Makeig, S. EEGLAB: An open source toolbox for analysis of single-trial EEG dynamics including independent component analysis. *J. Neurosci. Methods* **134**, 9–21 (2004).
101. Chang, C.-Y., Hsu, S.-H., Pion-Tonachini, L. & Jung, T.-P. Evaluation of artifact subspace reconstruction for automatic artifact components removal in multi-channel EEG recordings. *IEEE Trans. Biomed. Eng.* **67**, 1114–1121 (2020).
102. Cohen, M. X. *Analyzing Neural Time Series Data: Theory and Practice* (The MIT Press, 2014).
103. Chen, C. C., Henson, R. N., Stephan, K. E., Kilner, J. M. & Friston, K. J. Forward and backward connections in the brain: A DCM study of functional asymmetries. *NeuroImage* **45**, 453–462 (2009).
104. Furl, N., Coppola, R., Averbeck, B. B. & Weinberger, D. R. Cross-frequency power coupling between hierarchically organized face-selective areas. *Cereb. Cortex* **24**, 2409–2420 (2014).
105. Sanders, R. D. et al. Propofol-induced unresponsiveness is associated with impaired feedforward connectivity in cortical hierarchy. *Br. J. Anaesth.* **121**, 1084–1096 (2018).
106. van Wijk, B. C. M., Litvak, V., Friston, K. J. & Daffertshofer, A. Nonlinear coupling between occipital and motor cortex during motor imagery: A dynamic causal modeling study. *NeuroImage* **71**, 104–113 (2013).
107. Rosalyn J., Mkael, M., Symmonds Raymond J., Dolan Karl J., & Friston. The Brain Ages Optimally to Model Its Environment: Evidence from Sensory Learning over the Adult Lifespan PLoS Computational *Biology* **10**(1), e1003422 https://doi.org/10.1371/journal.pcbi.1003422 (2014).

Acknowledgements

Author contributions

Conceptualization, A.G.L., W.E.D, B.G.C, P.P.G and P.M.C.; Methodology, A.G.L. and W.E.D.; Data acquisition. A.G.L., L.Z.R. and B.G.C.; Data analysis, A.G.L., W.E.D., L.Z.R. and P.P.G.; Writing the manuscript, A.G.L. and W.E.D.; All authors reviewed the manuscript.

Competing interests

The authors declare no competing interests.

Additional information

Supplementary Information The online version contains supplementary material available at https://doi.org/10.1038/s41598-024-72229-x.

Correspondence and requests for materials should be addressed to A.G.-L.

Reprints and permissions information is available at www.nature.com/reprints.

Publisher's note Springer Nature remains neutral with regard to jurisdictional claims in published maps and institutional affiliations.